WING IN GROUND EFFECT - A NEW APPROACH FOR THE HUMAN POWERED HELICOPTER

A. Krenik, J. Götz
DLR Institute of Flight Systems, 38108 Braunschweig, Germany

Abstract

In this paper a brief overview of the human powered flight will be given at the beginning. The power demand of the most successful human powered fixed wing aircraft will be shown in order to point out the available power problems concerning the design of the rotary wing aircraft. The human ability to perform physical work and therein involved metabolic mechanisms will be shown with their limitations and problems in the accessibility for reliable human power expectations. Furthermore it is not possible to predict the duration of the increased power setting following the constant performance duration. The presentation of analytical calculation method of simplified helicoid will serve as an introduction to the main problem of human powered helicopters – the limited human power source. The invalidity of the common in ground effect models for the purpose of power demand estimation and modest success of realized human powered helicopter designs lead to the alternative approach – the wing in ground effect – as the most promising idea.

1. NOMENCLATURE

c	chord
c_d	drag coefficient
c_l	lift coefficient
$c_{l\alpha}$	lift curve slope
c_p	pressure coefficient
c_r	resultant force coefficient
c_t	thrust coefficient
c_q	tangential drag coefficient
c_T	rotor thrust coefficient: $T/(\rho S U^2)$
h	rotor height above ground
$\overline{h}$	nondimensional rotor height above ground: h/R
$\widehat{h}$	nondimensional rotor height above ground: h/c
k_{aerob}	constant of aerobic power
$k_{anaerob}$	constant of anaerobic power
l	coffset between inner and outer helices
m	mass
$\dot{m}$	mass flow
n_b	number of blades
p	screw pitch, pressure
r	radial coordinate
$\overline{r}$	nondimensional radial coordinate: r/R
s	angular screw pitch: $p/(2\pi)$
t	time
t_*	duration
w	air velocity through rotor disc plane
w_i	induced velocity in the rotor disc plane
D	drag
FM	figure of merit
P	induced power
P_{real}	real rotor power
P_H	human power
Q	torque
R	rotor radius, resultant force
S	surface area
T	thrust
U	tangential speed: Ωr
V	resultant velocity
V_{air}	airspeed
V_{max}	maximum shortening velocity of a muscle
$\dot{V}_{O_2}$	oxygen consumption
α	angle of attack
δ	anhedral angle between two helices
ε	erecting angle
φ	induced angle
λ_{aerob}	constant of aerobic power gain
$\lambda_{anaerob}$	constant of anaerobic power decay
θ	pitch angle
ρ	air density
σ	rotor solidity: $n_b c/(\pi R)$
τ	taper angle of the outer helix
ψ	azimuth angle
Ω	angular speed
Ψ	swept angle of the helicoid
$(\,)_\infty$	out of ground effect influence
CFD	computational fluid dynamics
HPA	human powered aircraft
HPH	human powered helicopter
IGE	in ground effect
OGE	out of ground effect

2. INTRODUCTION

The first drafted ideas of a machine, which should be able to produce lift only under exploitation of human strength to overcome its own weight and that of the human body, presumably go back on the Italian Leonardo da Vinci. Among other drawings one of his most famous sketches is the helicoid, which became a symbol of rotary wing aircraft. The sketch does not replicate nature's inventions, like the flapping wing of the bird flight, but its original idea can be found in the *Archimedes' Screw*. Today it seems to be obvious that this machine will never lift off under aid of human strength and only has the character of an artistic fiction.

In contrast to that, the human powered flight with fixed wing aircraft is no longer a utopia. It was proven possible nearly 75 years ago and attained substantial success in the 1980s. Inspired from these achievements the *Sikorsky Prize* has been offered in 1980 as an equivalent call for rotary wing aircraft. The main but still not fulfilled criteria are one minute hover and one single pull up to 3 meters above the ground. Until today only modest success has been made by more than a dozen of projects. Almost every possible rotor configuration has been considered (FIG 2). But only five[1] designs succeeded in hovering at least for a very short period of time.

The challenge of human powered flight was first met successfully by the Italians E. Bossi and V. Bonomi[2] in the 1930s. Their muscle-propelled motor glider named *Pedaliante* was able to perform a take-off and fulfilled a flight distance of 91 meters. About 40 years later the *First Kremer Prize* was won by the human powered aircraft (HPA) *Gossamer Condor*, reaching the requirements of completing a flight path in the shape of a horizontal eight around two pylons separated by 800 meters distance in less than 8 minutes flight time. The more challenging requirements of the *Second Kremer Prize* (i.e. crossing of the British Channel, covering a distance of 35.8 km) were also achieved in 1979. The best performance of human powered flight has so far been shown by the *Daedalus-Project* covering 115 km distance in less than 4 hours during a continuous flight. It is not surprising that the pilot of the *Daedalus-88* HPA was a professional world class cyclist. This, together with the application of ultra-light design and intensive research led to such a remarkable performance.

One of the challenges in designing a human powered helicopter (HPH) is the excessive demand for induced power due to lack of translational lift. To moderate this demand, the utilization of ground effect was understood as necessary from the beginning on. A fixed wing aircraft has only one possibility to lower the necessary power demand: increasing the airspeed. FIG 1 shows the calculated power curve of the *Daedalus-88* in horizontal flight. After applying the energy method, basically summarizing the drags of all aerodynamic components with the accessible data like weights, geometry and aerodynamics, the calculated results are fairly accurate compared to the published performance data [1].

[1] *da Vinci III* (1988), *Yuri I* (1994), *Gamera I* (2011), *Gamera II* (2012), *Upturn* (2012)

[2] The Germans H. Häßler and F. Villinger had a similar design *HV-1* in 1935, but it wasn't able to take off without a catapult.

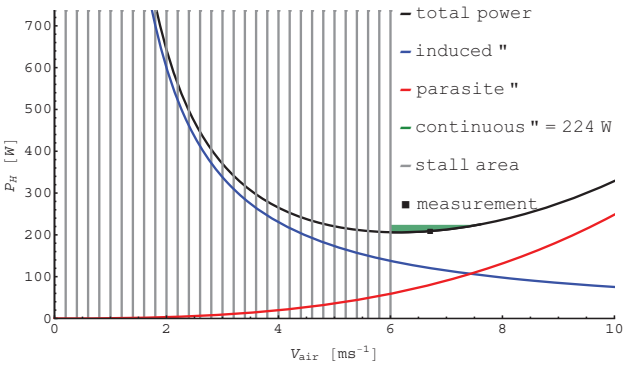

FIG 1. Calculated power curve of the *Daedalus-88* HPA

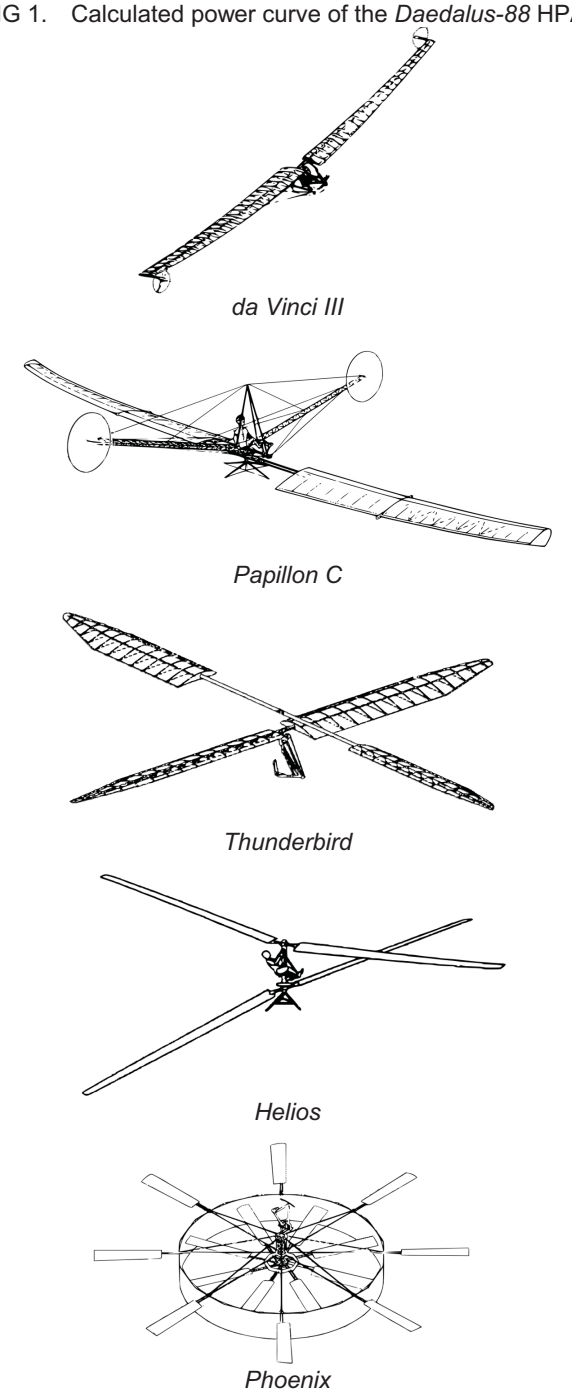

FIG 2. Sketches [2] of selected HPH projects

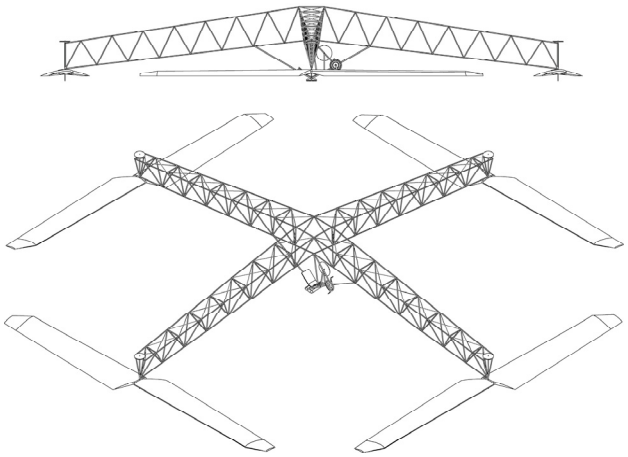

FIG 3. Sketch of *Yuri I* HPH [2]

The hyperbolic decrease of induced power with increasing airspeed is also existent for helicopters, but a design of a forward flying helicopter would unavoidably lead to more structural weight to meet all the requirements of dynamic stability and design strength. In addition, the forward flight would conflict with the regulations of the *Sikorsky Prize*[3]. Thus, the only way for HPHs to reduce the induced power and to have a chance to win the prize is to get in the operational area of the ground effect, or even more, the extreme ground effect.

The green filled area above the power curve marks the measured continuous power of 224 W (available to perform the 4 hours flight) of the pilot K. Kanellopoulos. It is obvious that the flight envelope of this aircraft was[4] very limited. The pilot could maintain the airspeed of 6.71 ms^{-1} providing 211 W [1] (209 W calculated). This context might illustrate how sparse the power reserves are even under best circumstances to continue the forward motion of a muscle-driven airplane, not to mention the difficulties considering the design of a hovering rotary wing aircraft.

To the present day many HPH-designs have been designed, but only five of them were able to lift off. The first successful human powered helicopter *da Vinci III* with one tip-driven, two-bladed lifting rotor performed a 7 seconds hover in 1989. The *Papillon C* (FIG 2) is the only design with antitorque rotors. All coaxial rotor designs (e.g. *Thunderbird*, *Papillon A*, *Papillon B*) failed to hover, or even broke apart in the attempt. The official world record holder with almost 20 seconds hovering duration is still the quadrotor HPH *Yuri I* from 1994 under the aegis of A. Naito from the Nihon University (FIG 3).

In 2011 the *Gamera I* HPH from the University of Maryland performed a hover with a duration of 11.4 seconds, setting a female athletes world record of the Fédération Aéronautique Internationale [3]. The design of *Gamera* is very similar to that of *Yuri I*, but some improvements were implemented, such as the hand crank mechanism in addition to the common pedals. Team *Gamera* is currently preparing the successive design to achieve the 60 seconds hover, as a prior step to the objective *Sikorsky Prize*. The team also carefully selected a group of male athletes with an optimum power to body mass ratio. A prior series of OGE- and IGE-tests with model and thereafter full scale rotors, led to the, within the considered design space, most advantageous shape of the used rotor blades [4]. The first flight tests were performed in June 2012, setting an unofficial record of 50 seconds in hover.

This paper contains two main parts. In the first, the human performance will be described as far as it is of interest for the design. In the second part, three rotary wing concepts will be addressed, concerning their applicability as a human powered helicopter.

3. HUMAN PERFORMANCE

In contrast to an internal combustion engine or an electric motor, the ability of the human musculature to perform physical work is conditioned by many outward and individual factors. Characteristic above all is the qualitative dependence of the achievable power magnitude compared to the delivered constant power duration and the maximum strength as a function of the muscle contraction speed.

3.1. Power-Dependent Energy Allocation

The basis of muscle work are complicated muscle fiber contractions. The necessary energy is provided in form of the adenosine triphosphate molecule (ATP), which can be seen as an intercellular energetic unit of currency. The amount of ATP stored in the muscles is very limited (approx. 5µmolg^{-1} muscle) and is sufficient for only very few muscle contractions. As a consequence it has to be resynthesized continuously [5].

ATP synthesis occurs through four metabolic processes:

- Hydrolysis of phosphocreatine (PCr)
  - anaerobic energy pathway
  - approx. 10-20 seconds duration limit
- Glycolysis
  - anaerobic energy pathway
  - approx. 4 minutes duration limit
- Oxidation of carbohydrates
  - aerobic energy pathway
  - approx. 100 minutes duration limit
- Oxidation of fatty acids
  - aerobic energy pathway
  - duration limit is about days

Depending on demanded muscle power delivery and output duration different metabolic processes may take place in parallel. Mechanical power delivery within the range of maximum endurance (200-250 W for a few hours) is achieved very quickly and can be sustained for hours. The necessary oxygen consumption however rises slower than the set up energy demand and needs about three minutes to reach the stationary value (steady-state). Therefore the O_2-deficiency has to be bridged by the two other anaerobic energy delivering processes (FIG 4) and afterwards the O_2-debt has to be amortized. The O_2-deficiency depends on the provided physical performance and is non-linear. The amount of the O_2-debt is generally less among trained individuals due to bigger stroke volume and the higher degree of muscle capillarization. In general, the amount of the O_2-debt is bigger compared to the O_2-deficiency. The context of ATP-synthesis with aerobic and

[3] The hover should be maintained within a 10 m by 10 m square.
[4] The aircraft broke apart 30 meters from the finish line shore.

anaerobic metabolic processes can be seen in FIG 5, where the ATP-concentration remains nearly constant to maintain the constant physical power output.

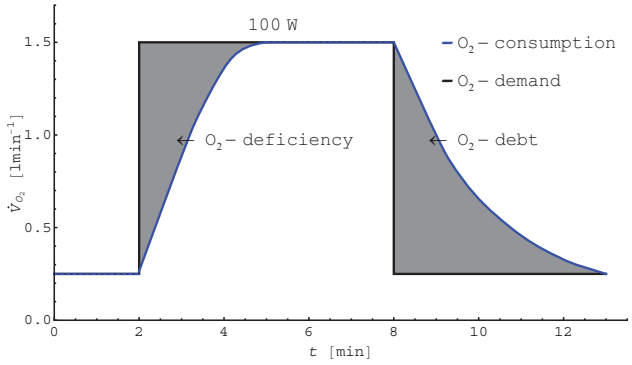

FIG 4. O_2-deficiency and O_2-debt (from [5])

At the same time the level of phosphocreatine drops from the initial state and the mentioned slowly rising O_2-consumption reaches the steady state after only three minutes of physical performance, relieving the hydrolysis of phosphocreatine until both processes stabilize.

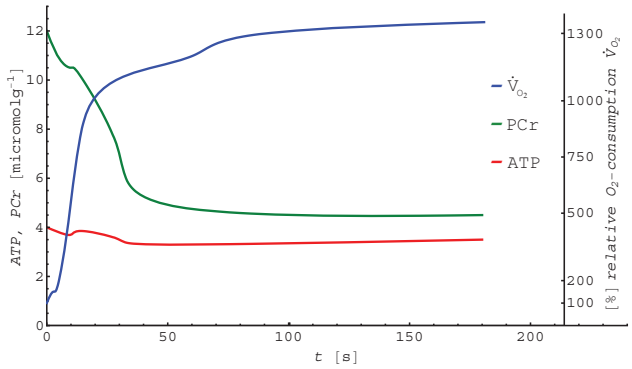

FIG 5. Interchange of anaerobic and aerobic processes (from [5])

Depending on the magnitude of the physical power output the steady-state of the oxygen-consumption may not be reached, while the anaerobic energy sources will quickly exhaust, leading to the collapse of the human efforts.

3.2. Human Power Potential

The ability of the human body to perform physical work is based on application of forces through muscle contraction. Muscle shortening velocity, as the governing mechanism, depends on the applied force and corresponds to the load. Unloaded, the muscle contracts with the maximum velocity V_{max}. With increasing load the muscle contraction velocity decreases hyperbolically leading to the maximum value of the generated force at zero mechanical work and thus performing no physical power. This relationship is summarized in the *Hill Curve* [5] in FIG 6. The maximum power is in the area of 20-30% of the maximum applied force and 30-35% of the maximum shortening velocity. This correlation is not negligible in the dimensioning of gear transmission ratios of pedal and hand crank devices.

One of the first to study the application of different workout devices in the field of human powered aircraft was O. Ursinus [6]. He came to the conclusion that the best device to exploit the human power is a combination of pedals and a hand crank mechanism. Some of his results were assembled by D. Wilkie [7] (FIG 7). The spreading of the measurements can be explained by the fact that the tests were conducted with different individuals that were separated in four groups.

- Normal healthy male individuals
  - only pedaling
- Normal healthy male individuals
  - pedaling and using arms
- World class male athletes
  - only pedaling
- World class male athletes
  - pedaling and using arms

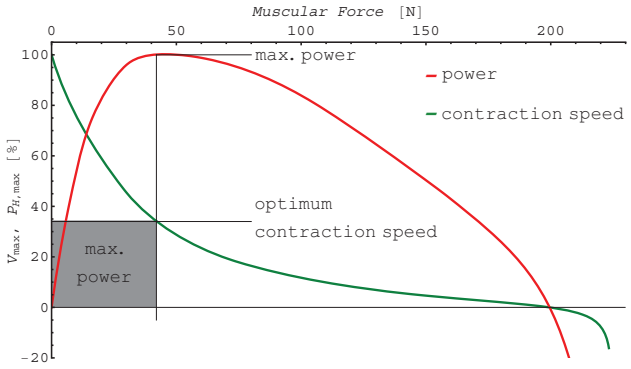

FIG 6. Dependency of mechanical power on muscular force (load) and contraction speed

The measurements can be fitted with the following formula:

$$P_H = k_{aerob}\left(1 - e^{-\lambda_{aerob} t_*}\right) + k_{anaerob} e^{-\lambda_{anaerob} t_*} \quad (1)$$

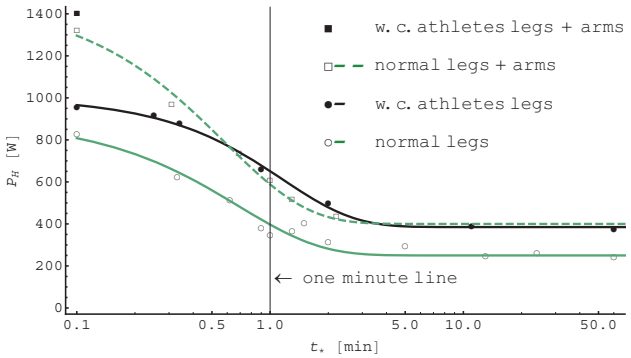

FIG 7. Measurements of constantly delivered power output in dependency on exercise duration

The equation represents the alteration between the aerobic and anaerobic energy sources. The boundary values are the maximum power available for the shortest period of the exercise, which is $k_{anaerob}$, and the maximum continuous power k_{aerob} respectively. The parameters of the fitted curves are collected in TAB 1.

	k_{aerob} [W]	$k_{anaerob}$ [W]	λ_{aerob} [min^{-1}]	$\lambda_{anaerob}$ [min^{-1}]
□– –	400	1465	2	1.80
•–	385	1005	2	1.15
○–	250	895	2	1.60

TAB 1. Fitted parameters of power equation (1)

At the target hover duration of one minute there is only about half of the power available compared to the shortest power delivery of six seconds. An athlete driving the human powered helicopter, which is designed to hover with the power available for one minute, will not be able to perform the desired climb. For this reason the hover design point should be somewhere behind the one minute line. But there is no information about the power reserves if the athlete does not reach the maximum exercise duration to trade the left time (in other words left energy) for increased power setting but for a shorter duration.

The only way to make a statement about the ability of the HPH to meet the requirements of the *Sikorsky Prize* using this kind of power duration measurements is to calculate the power requirements of one minute climb with constant power to three meters height.

4. THE HUMAN POWERED ROTARY WING CONCEPTS

One possibility to give a machine airborne ability without translational motion is to provide the lift generating surfaces the possibility of rotatory movements. Today, this insight is not too astonishing; in the Middle Ages and thus long before the first successful motorized flight this idea must have been revolutionary.

4.1. Leonardo da Vinci's Helicoid

From the very often used drawing of *Leonardo da Vinci's Screw* a freely interpreted 3D-model was created to appraise the overall weight of such a construction[5] (FIG 8).

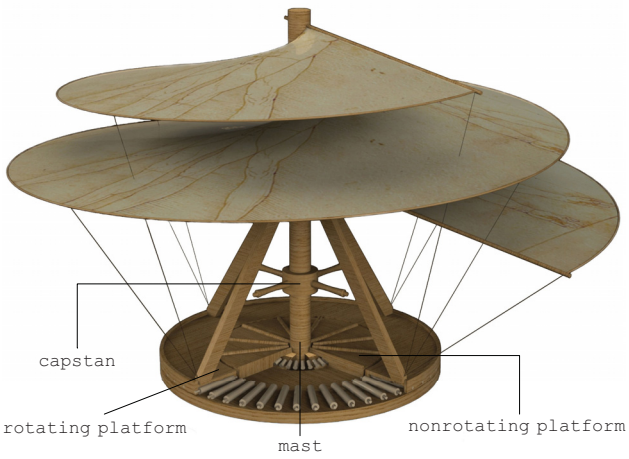

FIG 8. *da Vinci's Screw* as a freely interpreted 3D-model

[5] This computer aided design model, assuming it would be made of wood, would weigh about 2300 kg.

In this model, each of up to four men would have to lean and move against the capstan with four levers connected to the central mast, pushing themselves around from the central nonrotating platform. This platform would be fixed as long as the created lift does not reduce the frictional torque of the supporting lower platform. By neglecting these circumstances and thus imagining the contact area as fixed to the ground and thus unaffected by the created torque, the question of the applicability of this screw as a human powered device, which is able to lift its own weight, can be answered with the following approach.

In the first step the geometry of the (circular) helicoid must be accurately described in a suitable[6] coordinate system. After that, airflow forces can be applied to the infinitesimal surface elements and integrated.

Since the geometry of the mentioned *da Vinci's* drawing is more complex (FIG 9) than that of the standard helicoid, because of the tapered shape of the screw's silhouette and the anhedral angle between the inner and outer helices, these angles will be set to zero. The result is a simple helicoid with the center of area coinciding with the mast axis (FIG 10).

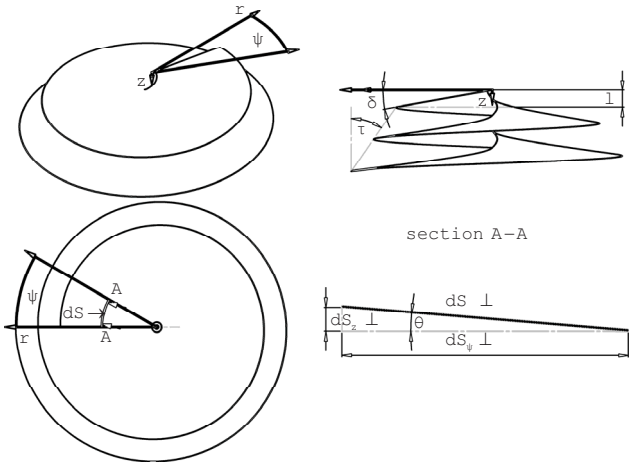

FIG 9. Description of the tapered and anhedral helicoid with cylindrical coordinates

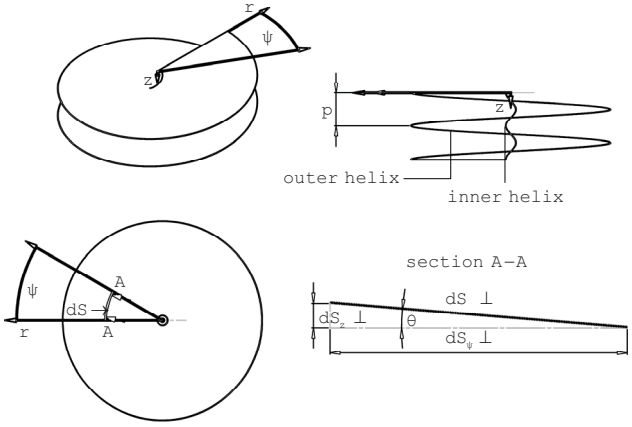

FIG 10. Description of the simple helicoid with cylindrical coordinates

[6] Basically this is a cylindrical coordinate system

Considering the geometric dependencies of the rolled out circular section A-A from FIG 11 the projected infinitesimal areas are:

$$dS_z = dr\,dz = dr\frac{p}{2\pi}d\psi = s\,dr\,d\psi \tag{2}$$

$$dS_\psi = r\,dr\,d\psi \tag{3}$$

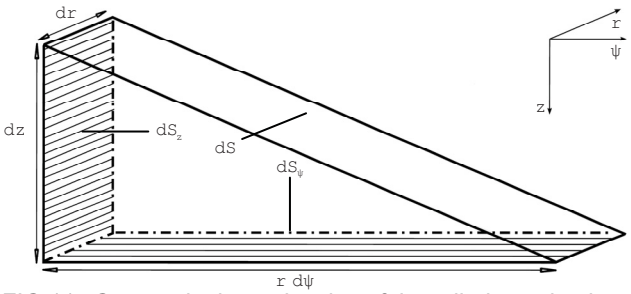

FIG 11. Geometric dependencies of the rolled out circular section

And the hypotenuse infinitesimal area respectively:

$$\begin{aligned} dS^2 &= dS_z^2 + dS_\psi^2 \\ &= s^2\left(dr\,d\psi\right)^2 + r^2\left(dr\,d\psi\right)^2 \\ &= \left(s^2 + r^2\right)\left(dr\,d\psi\right)^2 \\ dS &= \sqrt{s^2 + r^2}\,dr\,d\psi \end{aligned} \tag{4}$$

The overall curved area can be calculated from this analytically:

$$\begin{aligned} S &= \int_0^{\Psi}\int_0^{R}\sqrt{s^2 + r^2}\,dr\,d\psi \\ S &= \frac{\Psi}{2}\left(R\sqrt{s^2 + R^2} + s^2\ln\left(\frac{R + \sqrt{s^2 + r^2}}{s}\right)\right) \end{aligned} \tag{5}$$

Now imagining a free flow and applying the principles of linear momentum of section A-A in FIG 12 the resultant force dR is:

$$dR = \rho U^2\cos(\varepsilon)\,dS_z \tag{6}$$

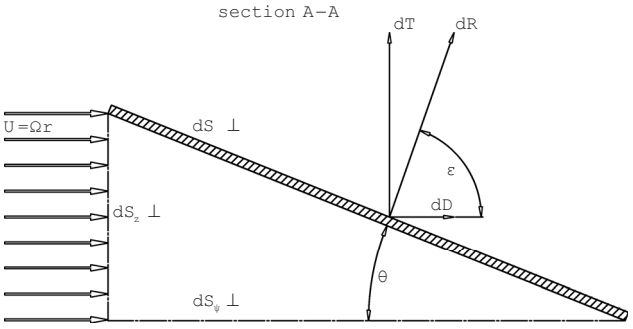

FIG 12. Circular section of the helicoid with applied forces of the relative airflow

The vertical component (thrust) is then:

$$\begin{aligned} dT &= dR\cos(\theta) \\ dT &= \rho U^2\cos(\varepsilon)\cos(\theta)\,dS_z \\ dT &= \rho U^2\cos(\pi/2 - \theta)\cos(\theta)\,dS_z \\ dT &= \rho U^2\sin(\theta)\cos(\theta)\,dS_z \end{aligned} \tag{7}$$

The horizontal component (drag) is obtained by:

$$\begin{aligned} dD &= dR\sin(\theta) \\ dD &= \rho U^2\sin^2(\theta)\,dS_z \end{aligned} \tag{8}$$

The pitch angle of the section varies with the radius:

$$\theta(r) = \arctan\left(\frac{\frac{p}{2\pi}\psi}{r\psi}\right) = \arctan\left(\frac{s}{r}\right) \tag{9}$$

This modeling implies force development resulting from elastic collision of the airflow with the helicoid section. There is no friction considered, as can be seen after building of thrust and drag coefficients from equations (7) and (8):

$$c_t = \frac{dT}{\rho U^2 dS_z} = \sin(\theta)\cos(\theta) \tag{10}$$

$$c_d = \frac{dD}{\rho U^2 dS_z} = \sin^2(\theta) \tag{11}$$

In FIG 13 it is plausible that at zero pitch angle there is neither thrust nor drag, that the maximum thrust is reached at 45°, decreasing to zero at 90° while at the same time the drag reaches the maximum and so forth.

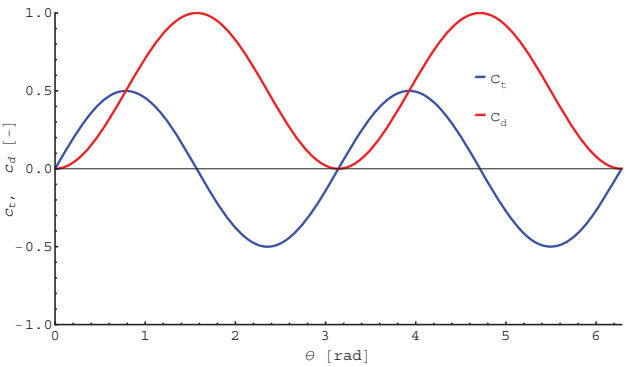

FIG 13. Thrust and drag of the helicoid section as a function of the pitch angle

With the preceding relations equation (7) can be rewritten in order to contain all the explicit variables and constants:

$$dT = \rho(\Omega r)^2 \sin(\theta)\cos(\theta)\, s\, dr\, d\psi$$

$$dT = \rho\Omega^2 r^2 s \sin\left(\arctan\left(\frac{s}{r}\right)\right)\cos\left(\arctan\left(\frac{s}{r}\right)\right) dr\, d\psi$$

(12)
$$dT = \rho\Omega^2 r^2 s \frac{s}{r\sqrt{1+\frac{s^2}{r^2}}}\frac{1}{\sqrt{1+\frac{s^2}{r^2}}} dr\, d\psi$$

$$dT = \rho\Omega^2 s^2 r \frac{1}{1+\frac{s^2}{r^2}} dr\, d\psi$$

The overall thrust of the simple helicoid with variable swept angle Ψ, radius R and angular screw pitch angle s can be calculated analytically with equation (12):

$$dT = \rho\Omega^2 s^2 r \frac{1}{1+\frac{s^2}{r^2}} dr\, d\psi$$

(13)
$$T = \rho\Omega^2 s^2 \int_0^{\Psi}\int_0^{R} \frac{r}{1+\frac{s^2}{r^2}} dr\, d\psi$$

$$T = \frac{\rho\Omega^2\Psi}{2}\left(R^2 + s^2 \ln\left(\frac{s^2}{R^2+s^2}\right)\right)s^2$$

A similar procedure can be applied to the drag, from which the more interesting required torque and hence the power will be obtained:

$$dQ = r\, dD$$

$$dP = \Omega r\, dD$$

(14)
$$dP = \Omega r \rho U^2 \sin^2(\theta) dS_z$$

$$dP = \rho\Omega^3 r^3 \sin^2\left(\arctan\left(\frac{s}{r}\right)\right) s\, dr\, d\psi$$

$$dP = \rho\Omega^3 r^3 \frac{s^3}{r^2+s^2} dr\, d\psi$$

Executing the double integration with the same boundaries as for the overall thrust, the power equation becomes:

(15)
$$P = \rho\Omega^3 \int_0^{\Psi}\int_0^{R} r^3 \frac{s^3}{s^2+r^2} dr\, d\psi$$

$$P = \frac{\rho\Omega^3\Psi}{2}\left(R^2 + s^2 \ln\left(\frac{s^2}{R^2+s^2}\right)\right)s^3$$

In the following it will be assumed that Leonardo da Vinci would have used the shape of the simple helicoid, rather than that based on his drawing. The complicated equations of the thrust and power of the tapered helicoid can still be evaluated, but probably only numerically. The geometrical parameters of the simplified 3D-model are:

- $R = 3\,\mathrm{m}$
- $\Psi = 4\pi$
- $p = 1\,\mathrm{m}$

It will be further assumed that four men are able to deliver one horsepower each. Thus, equation (15) will be evaluated in order to find the corresponding angular velocity Ω to the required power of 4 h.p. and after that equation (13) shows the generated thrust at this rotational speed (FIG 14):

- $P\left(\Omega = 22.145\ \mathrm{rads^{-1}}\right) = 4\ \mathrm{h.p.} = 2982.8\ \mathrm{W}$
- $T\left(\Omega = 22.145\ \mathrm{rads^{-1}}\right) = 86.3\ \mathrm{kg} = 846.3\ \mathrm{N}$

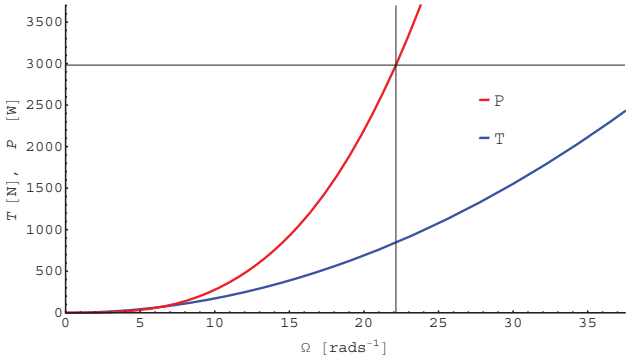

FIG 14. Thrust and required power of the simplified helicoid as function of the angular velocity

In total, the thrust is just about the weight of one man, but consuming the power of four.

4.2. Required Power Estimation of In Ground Effect Helicopters

All human powered helicopters which have been designed for the *Sikorsky Prize* applied the effect of increasing thrust of the rotor at constant power setting when approaching the ground surface. The effect can also be described as reduced power demand at constant thrust.

The mathematical tool of choice for the rough estimation of the rotor power demand is the actuator disk method including power reduction functions for ground effect modeling. But for more precise results the blade element method connected with reduction functions of the induced velocity should be used.

4.2.1. Actuator Disk Method

The easiest way to estimate the required power of a hovering helicopter is the application of the momentum theory, leading to the actuator disk method. The rotor power can be formulated as the rate of change of the kinetic energy between the plane far above the rotor disk ("0" in FIG 15) and the energy far underneath the rotor plane "2":

(16)
$$P = \frac{\dot{m}}{2}\left(w_2^2 - w_0^2\right) = \frac{\dot{m}}{2}\left(w_2^2 - 0\right)$$

The power is at the same time the product of thrust and the velocity in the rotor disk plane "1":

(17)
$$P = T\, w_1$$

The mass flow through the rotor disk plane "1" is:

(18) $$\dot{m} = \rho w_1 S$$

The rotor thrust is determined as the product of the air mass flow and the velocity increase:

(19) $$T = \dot{m}\left(w_2 - w_0\right) = \dot{m}\left(w_2 - 0\right)$$

and with equation (18):

(20) $$T = \rho w_1 w_2 S$$

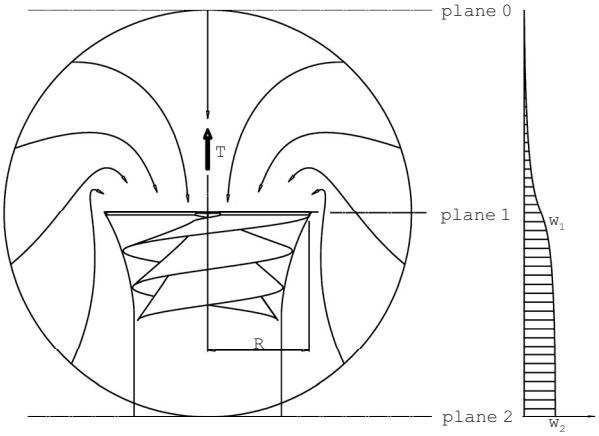

FIG 15. Side view of the actuator disk in hover

By inserting (17), (18) and (20) into (16), the induced velocity w_i in the rotor plane becomes:

(21) $$w_i = w_1 = \frac{w_2}{2}$$

With this relation the thrust can be written as:

(22) $$T = 2\rho w_i^2 S \Leftrightarrow w_i = \sqrt{\frac{T}{2\rho S}}$$

or including the power:

(23) $$T = \sqrt[3]{2\rho S P^2}$$

or finally, solved for the ideal (induced) power:

(24) $$P = \sqrt{\frac{T^3}{2\rho S}} = \sqrt{\frac{T^3}{2\rho \pi R^2}}$$

This equation does not contain the needed power, which is necessary to overcome the profile drag, nor does it consider the swirl losses and the flow unsteadiness due to the finite number of blades. It also presumes the constant distribution of the induced velocity[7]. To estimate realistic power demands the figure of merit with the optimistic value of 0.75 can be used:

(25) $$P_{real} = \frac{P}{FM} = \frac{1}{FM}\sqrt{\frac{T^3}{2\rho S}} = \frac{1}{0.75}\sqrt{\frac{T^3}{2\rho S}}$$

With it, it becomes possible to show that even under these favorable circumstances the necessary effort is hardly achievable by human beings (FIG 16).

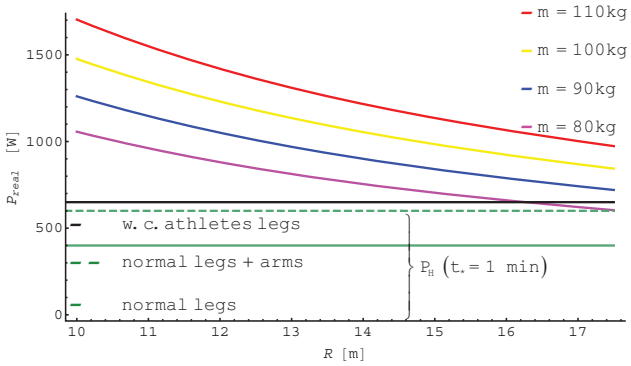

FIG 16. Required estimated rotor power for hover OGE compared to the 1 minute available power by human beings

4.2.2. Semi-Empirical IGE Methods

The well-known semi-empirical formulation of the in ground effect (IGE) thrust increase by I. Cheeseman and W. Bennett [8] are often used for the estimation of the required power. The relation can be written with (26) or without (27) the blade loading influence (c_T / σ):

(26) $$\left(\frac{T}{T_\infty}\right)_{P=const} = \frac{1}{1 - \frac{c_{l\alpha} w_i \sigma}{2\Omega R c_T}\left(\frac{R}{4h}\right)^2} = \frac{1}{1 - \frac{c_{l\alpha} w_i \sigma}{2\Omega R c_T}\left(\frac{1}{4\bar{h}}\right)^2}$$

(27) $$\left(\frac{T}{T_\infty}\right)_{P=const} = \frac{1}{1 - \left(\frac{R}{4h}\right)^2} = \frac{1}{1 - \left(\frac{1}{4\bar{h}}\right)^2}$$

A different estimation of the ground effect influence is the decrease of the induced power demand at constant thrust, which is based on the empirical formulation of the measurements database of J. Hayden [9]:

(28) $$\left(\frac{P}{P_\infty}\right)_{T=const} = f_H\left(\bar{h}\right) = \frac{1}{0.9926 + 0.15176\left(\frac{1}{\bar{h}}\right)^2}$$

The Cheeseman-Bennett method, as mentioned by the authors, delivers fairly accurate results down to $hR^{-1} \approx 0.5$. The Hayden method strongly underestimates the induced power below $hR^{-1} \approx 0.8$, as was shown by J. Light [10].

The considered maximum distance above the ground (3 meters) related to the variation of rotor radii of the designed and planned HPHs[8] leads to their operating area, which is out of the reliable boundaries of the two methods presented above (FIG 17, 18).

[7] The induced power consists of approx. 60% of the total necessary demand

[8] The variation of rotor radii is between 6 and 17.5 meters

Therefore the application of the common IGE-power estimation methods, as practicable for real helicopters, is not valid for the conditions of the human powered designs.

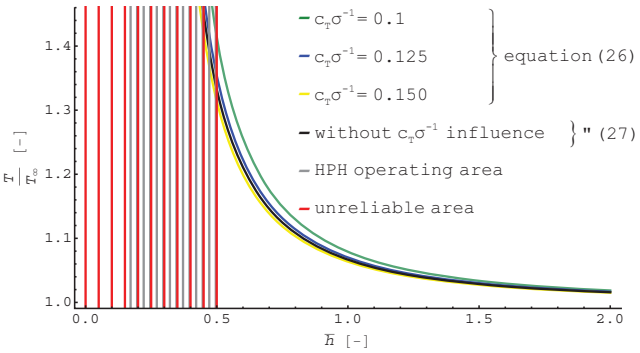

FIG 17. IGE thrust increase by Cheeseman-Bennett [8]

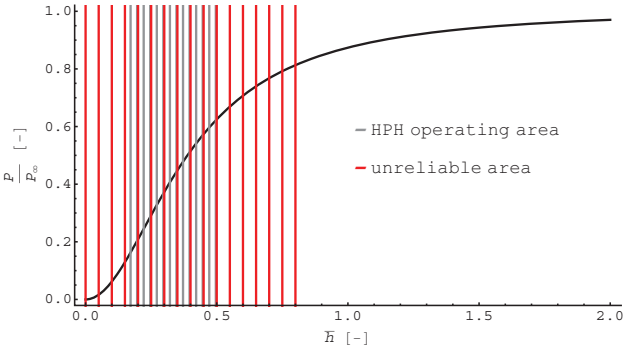

FIG 18. IGE induced power decrease by Hayden [9]

4.2.3. Blade Element Method with IGE Induced Velocity Distribution

The determination of the total rotor power with the blade element method (BEM) is possible to a higher degree of accuracy. The basic idea of BEM is the discretization of the rotor blade into elements with the following relations (FIG 19):

$$c_t = c_l\cos(\varphi) - c_d\sin(\varphi) \qquad (29)$$
$$c_q = c_l\sin(\varphi) + c_d\cos(\varphi)$$

with the effective angle of attack:

$$\alpha = \theta - \varphi \qquad (30)$$

and the corresponding resultant velocity at hover:

$$V = \sqrt{(\Omega r)^2 + w_i^2} \qquad (31)$$

The total thrust of the rotor results from the integration of all the vertical force components acting on the blade elements:

$$T = n_b c\frac{\rho}{2}\int_r V^2 c_t\, dr \qquad (32)$$

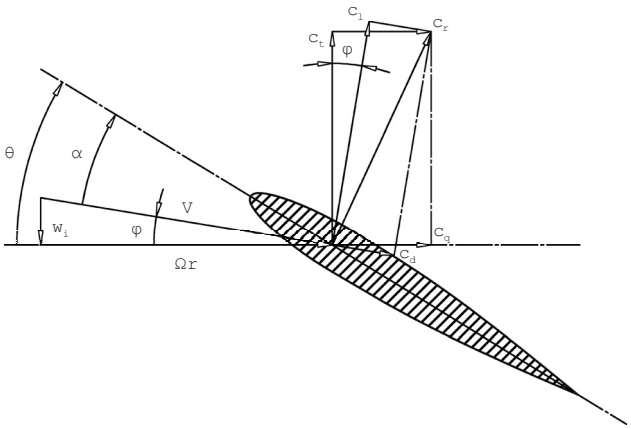

FIG 19. Forces and velocities at the moving blade element

With the same procedure the total rotor power can be obtained:

$$P = \Omega Q = \Omega n_b c\frac{\rho}{2}\int_r V^2 c_q\, r\, dr \qquad (33)$$

The blade element method works best when the aerodynamic data are provided in form of lookup tables. Another important key to the accuracy is the overlaid field of the induced velocities. In hover out of ground effect (OGE) and assuming ideally twisted blades the induced velocity is found in equation (22).

The span-wise distribution of the induced velocities, depending on the relative rotor height, can be calculated by means of numerically solving the equation formulated by M. Knight and R. Hefner [11]:

$$\frac{w_i}{w_{i\infty}} = f_{KH}\left(\bar{h},\bar{r}\right) = \frac{2\bar{h}}{\pi}\int_0^\pi \frac{1-\bar{r}\cos(\psi)}{1+\bar{r}^2-2\bar{r}\cos(\psi)}(A-B)\,d\psi$$
$$A = \frac{1}{\sqrt{1+\bar{h}^2+\bar{r}^2-2\bar{r}\cos(\psi)}} \qquad (34)$$
$$B = \frac{1}{\sqrt{1+4\bar{h}^2+\bar{r}^2-2\bar{r}\cos(\psi)}}$$

The calculated curves for some selected heights are shown in FIG 20.

It is possible to construct the power decrease function as in equation (28) with the ideal power and thrust relations from (22) and (24):

$$\left(\frac{P}{P_\infty}\right)_{T=const} = \frac{\sqrt{\left(2\rho S w_i^2\right)^3}}{\sqrt{\frac{T^3}{2\rho S}}} = \frac{\sqrt{\left(2\rho S w_i^2\right)^3}}{\sqrt{\left(2\rho S w_{i\infty}^2\right)^3}} = \left(\frac{w_i}{w_{i\infty}}\right)^3 \qquad (35)$$

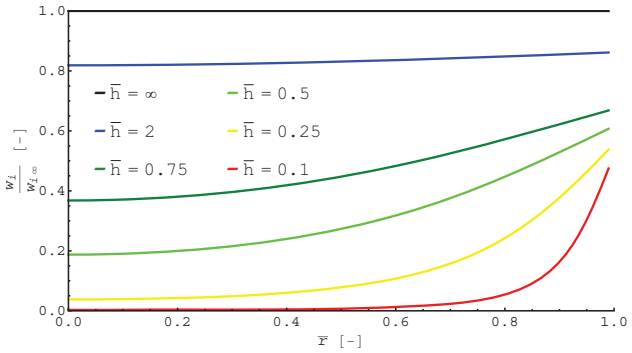

FIG 20. Decreasing radial distribution of the induced velocity with ground convergence by Knight and Hefner [11]

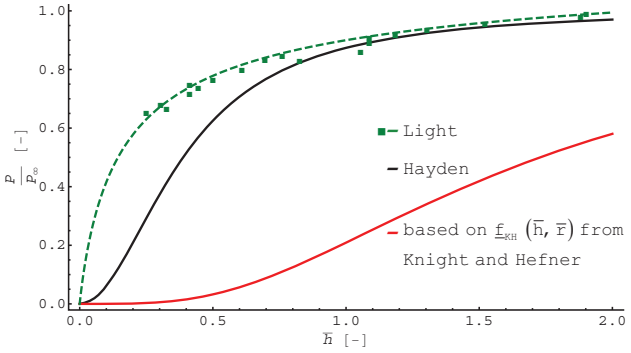

FIG 21. IGE induced power decrease by Light [10], Hayden [9] and the constructed trend based on Knight and Hefner [11]

Because the induced velocities of the Knight-Hefner equation are dependent on the rotor radius, the resultant function will be averaged prior to use in equation (35):

$$f_{KH}\left(\bar{h}\right) = \underline{f}_{KH}\left(\bar{h},\bar{r}\right) = \frac{1}{\bar{r}=\bar{R}}\int_0^{\bar{r}=\bar{R}} f_{KH}\left(\bar{h},\bar{r}\right)d\bar{r} = \frac{1}{1}\int_0^1 f_{KH}\left(\bar{h},\bar{r}\right)d\bar{r} \tag{36}$$

For the actual, height-dependent induced velocity in the numerator the averaged function from equation (36) is inserted into (35):

$$\left(\frac{P}{P_\infty}\right)_{T=const} = \frac{\sqrt{\left(2\rho S w_{i\infty}^2\left(f_{KH}\left(\bar{h}\right)\right)^2\right)^3}}{\sqrt{\left(2\rho S w_{i\infty}^2\right)^3}} = \frac{\sqrt{\left(2\rho S w_{i\infty}^2\left(f_{KH}\left(\bar{h}\right)\right)^2\right)^3}}{\sqrt{\left(2\rho S w_{i\infty}^2\right)^3}} = \left(f_{KH}\left(\bar{h}\right)\right)^3 \tag{37}$$

The resulting curve from equation (37) in FIG 21 is even more optimistic than Hayden's. The measurements with the lowest power decrease are those conducted by J. Light [10] with the following fitted formula:

$$\left(\frac{P}{P_\infty}\right)_{T=const} = f_L\left(\bar{h}\right) = \frac{-1.35}{0.05 - 0.2\,\bar{h}^{-0.95} - 1.35\,\bar{h}^{-0.05}} \tag{38}$$

Furthermore, the trend of reduction of the averaged induced velocity as a function of height can be obtained by calculation of the third root of any known (but from rotor radius independent) induced power function, as exemplarily shown in FIG 22:

$$\frac{w_i}{w_{i\infty}} = f(\bar{h}) = \sqrt[3]{\left(\frac{P}{P_\infty}\right)_{T=const}} \tag{39}$$

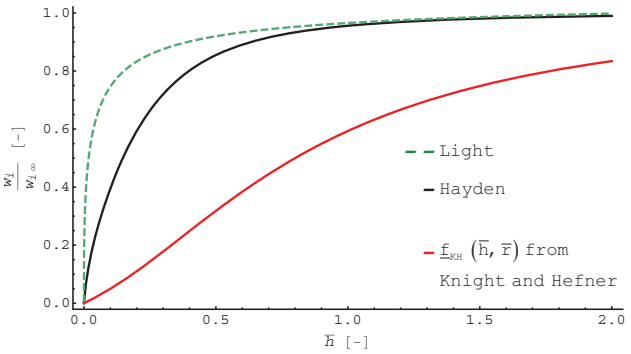

FIG 22. IGE induced velocity decrease from the induced power reduction trends by Light [10], Hayden [9] and Knight and Hefner [11]

More reliable in that case seem the curves by J. Light, in particular due to the measurements down to $hR^{-1}\approx 0.25$. But closer towards the ground the extrapolated curve remains speculative, especially in the context of contested portability of fast turning rotor measurements to the slow turning, as are present in HPH-designs. Thus, it becomes clear that there is no reliable theoretical method (except the detailed investigation with CFD methods) treating the extreme ground effect, or in the words of F. Harris [12]:

"…despite the theoretical work by Knight, Hefner, and Betz, rotor power in ground effect for a given thrust was strictly an empirical to semi-empirical engineering art. It was an art then and still is today, unfortunately…"

4.3. Wing in Ground Effect Helicopter

The wing in ground effect (WiG) has so far not been considered as a main design idea. In contrast to the rotor in ground effect the influence parameter is characterized by the increasing lift to drag ratio of a wing section in ground proximity, if the height is less than the chord length. Although A. Naito [13] mentioned the effect at least once as an unfavorable influence, it is certain that *Yuri I* operated in this area[9]. This might even be the main reason why *Yuri I* managed to hover at all.

The wing in ground effect has been applied to fixed wing aircraft, most notably the Russian-made ekranoplans. A characteristic of all WiG-aircraft is a very small aspect ratio

[9] The chord at the blade root was about 1 m and the height above ground 25 cm.

of the wings. Besides the very few available aerodynamic measurements of wings and airfoils under extreme ground conditions, there is extensive theoretical work of the last 30 years concerning the ground effect of such aerial vehicles by K. Rozhdestvensky [14], which does not treat rotary wings.

4.3.1. The Concept

The sketch of the wing in ground helicopter concept (FIG 23) differs a lot from the existing human powered helicopters, as the main design goal was a wide chord. The helicopter's inherent reaction torque problem might be solved with two antitorque rotors. The control of the blade pitch angle can be enabled with flap actuated canards. Their control links run through the rotor blade pitch axes in order to avoid kinematic couplings. The power input devices would consist of pedals and hand cranks. This leads to the unsolved problem how to manually control the helicopter while all human extremities are used for power generation.

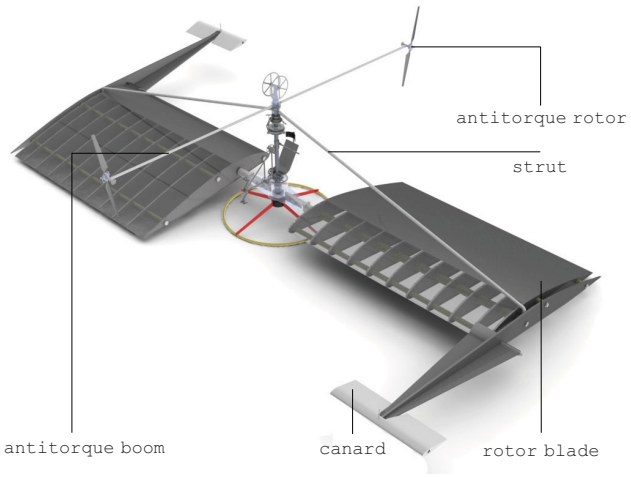

FIG 23. WiG-HPH-Concept

4.3.2. 2D Characteristics of Airfoils

The pressure distribution of a wing with infinite span changes dramatically with the approximation to the ground. Along the underside of the airfoil local flow decelerates, while the local pressure increases, forming some kind of dynamic aircushion underneath the wing:

$$c_{p,u} = \frac{p - p_\infty}{(\rho/2)V^2} \to 1 \tag{40}$$

The obtaining of 2-dimensional airfoil characteristics is possible with several accessible codes, such as *JavaFoil* [15] in a fairly good agreement with experimental data. In FIG 24 the calculated (with *JavaFoil*) pressure distribution of a modified CLARK-YH[10] airfoil is shown out of ground effect (top) and under extreme ground effect conditions (bottom). Considering the increased pressure distribution at the underside in the first half of the chord (FIG 24, bottom), it becomes identifiable that the additional lift results in a higher steepness of the lift curve slopes dependent on the height of the airfoil above the ground related to its chord (FIG 25). The calculated lift to drag ratios (FIG 26) show the quite impressive influence of the ground proximity. For the best performance the aimed angles of attack are those corresponding to maximum lift to drag ratios, which are for all heights in the range of 3 to 6 degrees.

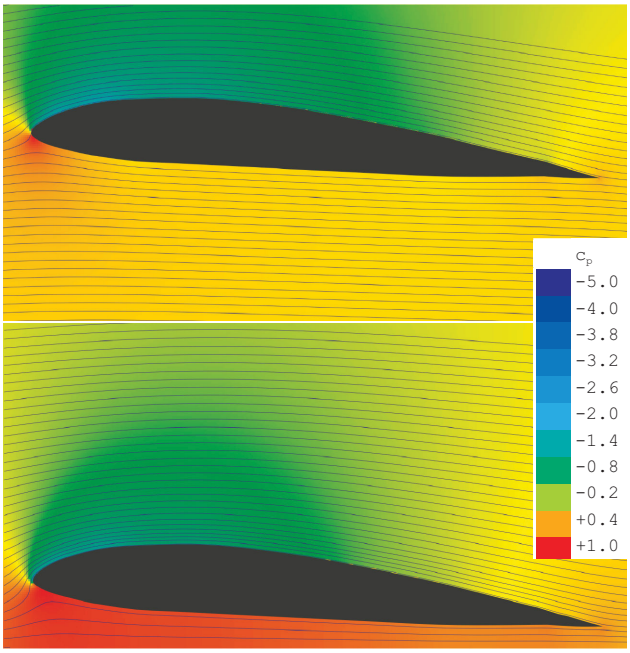

FIG 24. Pressure coefficient of CLARK-YH airfoil OGE (top) and IGE (bottom) at α=3°, h/c=0.05, Re=10^6

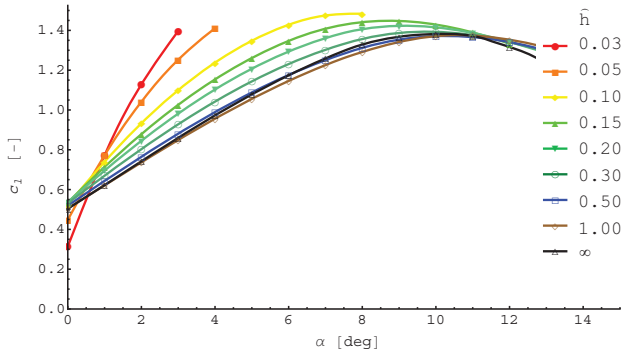

FIG 25. CLARK-YH lift coefficient in ground influence

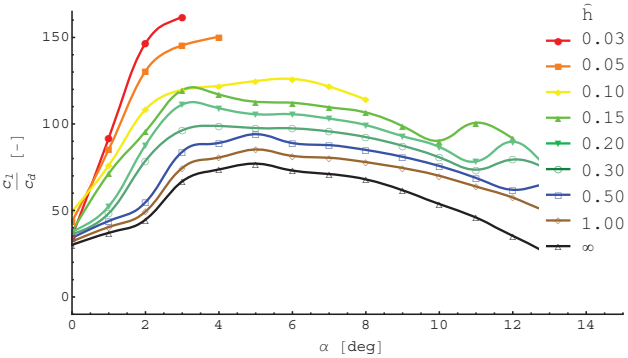

FIG 26. CLARK-YH lift to drag ratios in ground influence

[10] The aft 10 percent of the chord of the foil were flapped down by 5°.

4.3.3. 3D Problems of the WiG Application

There is no theoretical method at this time available for the application of the wing in ground effect to rotating wings. The power requirement for the most optimistic case can be calculated under the assumption of neglected inflow in extreme ground effect, as the trends of the curves in FIG 22 show. The power demand is calculated with the blade element method, using foil tables dependent on Reynolds number, height of the airfoil and angle of attack. The concept helicopter, as shown in FIG 23, is described with the following parameters:

- $\Omega = 1.5\pi \text{ rads}^{-1}$
- $R = 5 \text{ m}$
- $c = 3 \text{ m}$
- $\hat{h} = 0.05$
- $m = 100 \text{ kg}$

The resulting power, neglecting the power needed for the two antitorque rotors (which would consume approximately 10% of the main rotor power) is:

- $P(\theta = 3.275°) = 85 \text{ W}$

This result can be seen as the extremely optimistic value, since it does not consider the inflow, the blade tip losses and other power consuming effects of thrust generation. This value is about one fifth of the measured power of *Gamera II*, which recently succeeded in hovering for almost 50 seconds. Thus, this margin of the promising but uncertain power demand difference should be suitable for the motivation of further (experimental) investigations of the slowly rotating and small aspect ratio wings in extreme ground effect.

5. CONCLUSIONS

Referencing the first historical idea of a human powered helicopter by *Leonardo da Vinci* led to the mathematical description of his helicoid with the subsequent application of the elastic collision model with the aim of power demand estimation of the real-size construction. The calculated power demand of the helicoid, even under optimistic assumptions, is as expected very high and thus this screw device is rated as not suitable for the muscle driven lift generation and remains an ancient artistic fiction.

The display of the power demand curve of human powered fixed wing aircraft underlined the main component of the power requirement of a hovering rotor, the induced power demand, which the fixed wing aircraft can successfully surmount by means of moderate horizontal flight, but what the helicopter in the case of challenging the *Sikorsky Prize* is not allowed to do.

Although remarkable efforts and progress have been made in the field of the human powered helicopter performance in the past thirty years, only one requirement of the *Sikorsky Prize*, the one minute hover, seems to be achievable by the team of *Gamera II*. This discipline is hard enough to accomplish, but concerning the mandatory pull up to three meters height, the very scarce human power resources become evident. The only way to achieve the goal is to design a machine which is capable to hover as long as possible at such a low required power level that allows saving enough reserves for the ultimate climb effort. Consequently there are two main unknowns: on one hand the not yet documented human ability to perform a higher level of muscular power as a function of performance duration at some moderate level of exertion (this can be studied by sport physiologists) and on the other hand the lack of an accurate theory describing the extreme ground effect to predict the required power of the rotor as exactly as possible. The design of such a helicopter is engineering art. The application of the wing in ground effect might be the way towards realizing it.

6. REFERENCES

[1] Nadel, E. R., Bussolari, S. R., “The Daedalus Project Physiological Problems and Solutions”, American Scientist, Vol 76, 1988.
[2] http://www.humanpoweredhelicopters.org/
[3] Berry, B., Bowen-Davies, G., Gluesenkamp, K., Kaler, Z., Schmaus, J., Staruk, W., Weiner, E., Woods, B. K. S., et al., “Design Optimization of Gamera II: a Human Powered Helicopter”, 68th American Helicopter Society Forum, 2012.
[4] Schmaus, J., Berry, B., Gross, W., Koliais, P., “Experimental Study of Rotor Performance in Deep Ground Effect with Application to a Human Powered Helicopter”, 68th American Helicopter Society Forum, 2012
[5] Schmidt, R. F., Lang, F., “Physiologie des Menschen“, Springer-Lehrbuch, 2005.
[6] Ursinus, O., “Mitteilungen des Muskelflug-Instituts“, Nr.1, Nr.3, Flugsport, 1936.
[7] Wilkie, D. R., “Man as an Aero Engine”, Journal of The Royal Aeronautical Society, Vol. 64, 1960.
[8] Cheeseman, I. C., Bennett, W. E., “The Effect of the Ground on a Helicopter Rotor in Forward Flight”, Reports and Memoranda No. 3021, 1957.
[9] Hayden, J., “The Effect of the Ground on Helicopter Hovering Power Required”, 32nd American Helicopter Society Forum, 1976.
[10] Light, J. S., “Tip Vortex Geometry of a Hovering Helicopter Rotor in Ground Effect”, American Helicopter Society Vol. 38, 1993.
[11] Knight, M., Hefner, R., “Analysis of Ground Effect on Lifting Rotor”, NACA-TN-835, 1941.
[12] Harris, F. D., “Introduction to Autogyros, Helicopters, and Other V/STOL Aircraft”, NASA/SP-2011-215959, 2011
[13] Naito, A., “Unknown Problems in Human Powered Helicopter”, Int. Human-Powered Flight Symposium, 1994.
[14] Rozhdestvensky K. V., “Aerodynamics of a Lifting System in Extreme Ground Effect”, Springer, 2000
[15] www.mh-aerotools.de/airfoils/javafoil.htm/